

# Atrial Fibrillation Promotion With Long-Term Repetitive Obstructive Sleep Apnea in a Rat Model



Yu-ki Iwasaki, MD, PhD,\*† Takeshi Kato, MD, PhD,\* Feng Xiong, PhD,\*‡ Yan-Fen Shi, MD,\* Patrice Naud, PhD,\* Ange Maguy, PhD,\* Kyoichi Mizuno, MD, PhD,† Jean-Claude Tardif, MD,\* Philippe Comtois, PhD,§ Stanley Nattel, MD\*†

## ABSTRACT

**BACKGROUND** Obstructive sleep apnea (OSA) importantly contributes to the occurrence of atrial fibrillation (AF) in humans, but the mechanisms are poorly understood. Experimental research has provided insights into AF promotion by acute OSA episodes. However, patients with OSA usually have frequent nocturnal episodes for some time before manifesting AF.

**OBJECTIVES** The goal of this study was to test the hypothesis that repetitive OSA causes cardiac remodeling that predisposes to AF.

**METHODS** We mimicked OSA by using a mechanical ventilator and closing the airway at end-expiration with a 3-way stopcock (OSA rats). Matched control groups included rats with the ventilator stopped but airway left open (open airway rats) and continuously ventilated rats (sham rats). OSA rats were exposed to 20 consecutive 2-min cycles of 40 s of apnea/80 s of ventilation per day, 5 days per week for 4 weeks.

**RESULTS** OSA significantly increased the duration of AF from (median [interquartile range]) 2.6 s [1.9 s to 8.9 s] (shams) and 16 s [1.8 s to 93 s] (open airway) to 49s [34 s to 444 s]. AF inducibility increased to 56% (9 of 16) of OSA rats; this is up from 15% (2 of 13) and 13% (2 of 15) in open airway and sham rats, respectively ( $p < 0.05$ ). OSA rats exhibited substantial atrial conduction slowing on optical mapping, along with connexin-43 down-regulation on both quantitative immunofluorescence (expression reduced by 58% vs sham rats) and Western blot (reduced by 38%), as well as increased atrial fibrous tissue content (by 71%). OSA also caused left ventricular hypertrophy, dilation, and diastolic dysfunction and enhanced AF inducibility during superimposed acute OSA episodes to 82.4% of rats.

**CONCLUSIONS** Chronically repeated OSA episodes cause AF-promoting cardiac remodeling, with conduction abnormalities related to connexin dysregulation and fibrosis playing a prominent role. This novel animal model provides mechanistic insights into an important clinical problem and may be useful for further exploration of underlying mechanisms and therapeutic approaches. (J Am Coll Cardiol 2014;64:2013-23) © 2014 by the American College of Cardiology Foundation.

Obstructive sleep apnea (OSA), characterized by repetitive interruption of ventilation during sleep caused by upper airway obstruction, is highly prevalent (1). Recent studies have implicated OSA as a significant risk factor for atrial fibrillation (AF) (2,3). Suggested potential pathophysiological mechanisms include hypoxia (4), negative intrathoracic pressure changes (5),

From the \*Department of Medicine, Montréal Heart Institute and Université de Montréal, Montreal, Quebec, Canada; †Department of Cardiovascular Medicine, Nippon Medical School, Tokyo, Japan; ‡Department of Pharmacology, McGill University, Montreal, Quebec, Canada; and the §Department of Physiology, Montréal Heart Institute and Université de Montréal, Montreal, Quebec, Canada. This project was funded by grants from the Canadian Institutes of Health Research (grant 6957) and the Heart and Stroke Foundation of Canada. The authors have reported that they have no relationships relevant to the contents of this paper to disclose.

[Listen to this manuscript's audio summary by JACC Editor-in-Chief Dr. Valentin Fuster.](#)

[You can also listen to this issue's audio summary by JACC Editor-in-Chief Dr. Valentin Fuster.](#)

Manuscript received April 1, 2014; revised manuscript received May 8, 2014, accepted May 26, 2014.



**ABBREVIATIONS  
 AND ACRONYMS**

- AF** = atrial fibrillation
- AV** = atrioventricular
- ERP** = effective refractory period
- LA** = left atrial
- LV** = left ventricular
- MAPK** = mitogen-activated protein kinase
- OSA** = obstructive sleep apnea
- PBS** = phosphate-buffered saline
- RA** = right atrial
- RV** = right ventricular

sympathovagal imbalance (6), and structural remodeling (7,8). We recently reported that negative intrathoracic pressure changes during acute obstructive apnea promote AF, primarily by causing acute left atrial (LA) dilation (9).

SEE PAGE 2024

Most patients with OSA experience repeated nocturnal OSA episodes. It is conceivable that such repeated events lead to cardiac remodeling. Indeed, patients with repetitive OSA exhibit LA dilation and left ventricular (LV) hypertrophy associated with AF occurrence (10,11). However, the long-term cardiac effects of repetitive OSA on atrial properties and AF susceptibility have not been studied in experimental models. The present study was designed to assess the long-term effects of repetitive OSA on cardiac structure/function and AF susceptibility in a rat model.

**METHODS**

Only the principal methods are provided here; the [Online Appendix](#) provides a detailed description of the methods.

**LONG-TERM OSA-MODEL.** Twelve-week-old male Sprague-Dawley rats were intubated and ventilated with 2% isoflurane/room air. Volume-controlled ventilation was delivered with a tidal volume and respiratory rate of 2.5 ml and 72 cycles/min, respectively. OSA was mimicked by closing the airway at end expiration for 40 s, followed by 80-s recovery periods, 20 consecutive times per day (Figure 1). After OSA cycles, rats were ventilated with room air during recovery from anesthesia and then extubated after confirming spontaneous respiration. No complications resulted from anesthesia, ventilation, or OSA. OSA cycles were repeated daily (5 days per week for 4 weeks). Two control groups were studied: 1) open airway rats subjected to the same ventilator-arrest cycles but without airway closure; and 2) sham rats ventilated with isoflurane/room air throughout the procedure. Animals in all 3 groups were subjected to daily oropharyngeal intubation for ventilation. No animal showed signs of complications of intubation such as stridor or tachypnea. After 4 weeks, in vivo electrophysiological studies and AF induction assessments were performed, and tissues were procured.

A 3-F pressure-transducer catheter (Scisense P-catheter; Scisense Inc., London, Ontario, Canada) was introduced into the esophagus close to the LA posterior wall to monitor intrathoracic pressure in 6 OSA rats and 5 open airway rats. For blood pressure monitoring, a 2-F pressure transducer catheter (Scisense P catheter-RAT) was introduced into the ascending aorta through the left internal carotid artery.

**IN VIVO ELECTROPHYSIOLOGICAL STUDY.** To measure effective refractory periods (ERPs), programmed right atrial (RA) stimulation was performed at a cycle length of 150 ms (pulse width 2 ms, 2 × threshold current). Atrial and atrioventricular (AV) conducting system ERPs were defined as the longest S1-S2 coupling interval failing to generate a propagated beat. To assess atrial tachyarrhythmia inducibility, 25-Hz burst pacing (pulse width 2 ms, 4 × threshold current) was applied for 3 s, with 6 3-s burst cycles separated by 1-s intervals. AF was defined as a rapid (>800 beats/min) irregular atrial rhythm, and AF inducibility was defined as AF lasting for at least 1 s immediately after the 6-burst cycle protocol. If AF was induced after <6 burst pacing cycles, burst pacing was suspended to avoid interfering with the evolution of the AF. AF duration was determined in each rat as the mean duration of all AF episodes. If burst pacing at baseline did not induce AF, the same pacing protocol was repeated during acute OSA. Wenckebach cycle length was defined by failure of

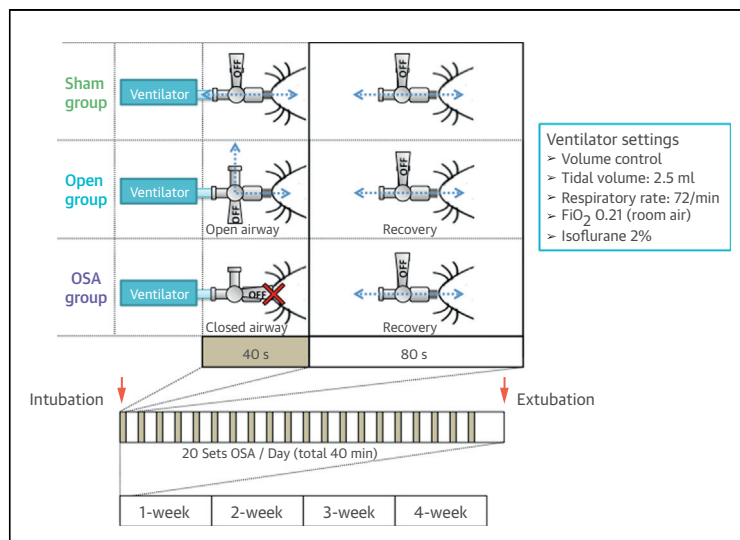


**FIGURE 1** Experimental Protocol

Sprague-Dawley rats were ventilated via an endotracheal tube connected to a 3-way stopcock. Obstructive sleep apnea (OSA) was mimicked by stopping the ventilator and closing the airway at end expiration for 40 s, followed by an 80-s recovery period (120 s/cycle). The 2-min cycle was repeated 20 times per day, 5 days per week for 4 weeks. The open airway group had the same cycles but with open (instead of closed) airways during apnea. The sham group was ventilated throughout the procedure. FIO<sub>2</sub> = fraction of inspired oxygen.

1:1 AV conduction, determined by RA pacing with decremental 5-ms steps. Sinus node recovery time was determined by 30-s RA pacing with a 150-ms cycle length.

**ECHOCARDIOGRAPHY.** Transthoracic echocardiographic studies were performed at baseline and after the 4-week preparation interval with a phased array 10S probe (4.5 to 11.5 MHz) in a Vivid 7 Dimension system (GE Healthcare Ultrasound, Horten, Norway), under sedation with 2% isoflurane. The [Online Appendix](#) presents details regarding the echocardiographic methods.

**PROTEIN EXTRACTION AND WESTERN BLOT.**

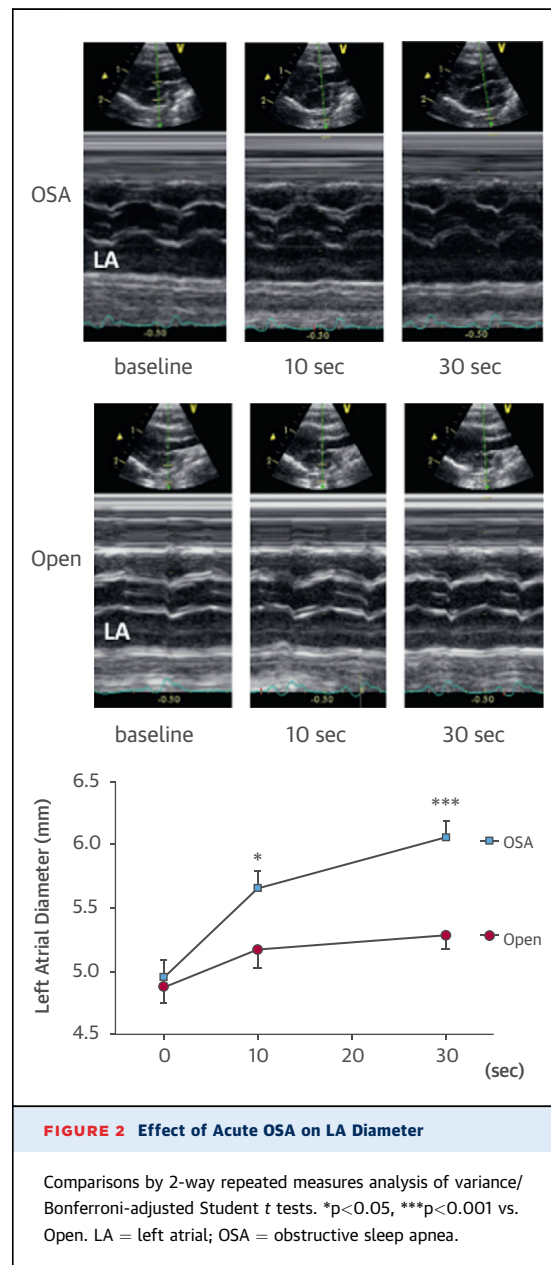
Freshly isolated LA samples were snap-frozen in liquid nitrogen and mechanically homogenized in TNE (Tris-NaCl-EDT) buffer containing the following: Tris 25 mmol/l, EDT (ethylenediaminetetraacetic acid) 5 mmol/L, EGTA (ethylene glycol-bis[2-aminoethylether]-N,N,N',N'-tetraacetic acid) 5 mmol/l, NaCl 150 mmol/l, NaF 20 mmol/l, Na<sub>3</sub>VO<sub>4</sub> 0.2 mmol/l,  $\alpha$ -glycerophosphate 20 mmol/l, AEBSF (4-[2-Aminoethyl]benzenesulfonyl fluoride hydrochloride) 0.1 mmol/l, leupeptin 25  $\mu$ g/ml, aprotinin 10  $\mu$ g/ml, pepstatin 1  $\mu$ g/ml, microcystin-LR 1  $\mu$ mol/l, pH 7.34, and hydrochloric acid. Homogenized samples were centrifuged at 1,000  $\times$  g for 10 min, and supernatant was collected and ultracentrifuged at 100,000  $\times$  g for 1 h. The resulting cytosolic fraction supernatant was kept for mitogen-activated protein kinase (MAPK) study. The membrane fraction pellet was incubated in TNE buffer containing 1% Triton-X100 for connexin-43 analysis. The protein concentration was determined with Bradford assay (Bio-Rad Laboratories, Inc., Hercules, California). All of the aforementioned steps were conducted on ice at 4°C to 5°C.

Protein samples (20  $\mu$ g) were separated by electrophoresis on 8% sodium dodecyl sulfate polyacrylamide gels and transferred electrophoretically onto polyvinylidene difluoride membranes. These membranes were blocked in a phosphate-buffered saline (PBS) containing 0.05% (volume/volume) Tween-20 and 5% (weight/volume) nonfat dry milk and incubated overnight at 4°C with primary antibodies diluted in PBS containing 0.05% Tween-20 and 1% nonfat dry milk. After washing with PBS-Tween/1% nonfat dry milk, membranes were hybridized with horseradish peroxidase-conjugated secondary antibody. Immunoreactive bands were detected by electrochemiluminescence by using BioMax MS/MR films. Protein quantification was performed with Quantity One software (Bio-Rad). All expression data are relative to glyceraldehyde-3-phosphate dehydrogenase staining for the same samples on the

same gels. The [Online Appendix](#) presents detailed information about antibodies, including sources and concentrations.

**HISTOLOGY.** Sections (5  $\mu$ m) were cut at room temperature and stained with Masson's Trichrome. Stained images were digitized and the fibrosis area was analyzed by using ImageJ 1.45s software. Fibrosis was quantified by a blinded observer and expressed as percent cross-sectional area, excluding blood vessels and perivascular tissue.

**CONFOCAL IMAGING.** Cryosections (14  $\mu$ m) were fixed with PBS containing 4% paraformaldehyde (pH



7.34), blocked, and permeabilized with PBS containing 2% normal donkey serum and 0.5% Triton X-100. Primary antibodies (mouse anti-Cx43 [Chemicon]; rabbit anti-Cx40 [Zymed]) were diluted (1/200) in PBS containing 2% normal donkey serum and 0.1% Triton X-100 for overnight incubation with cryosections. Alexa Fluor-conjugated donkey anti-rabbit (488 nm, Invitrogen) or donkey anti-mouse (555 nm, Invitrogen) were used as secondary antibodies (1/600 dilution). Alexa Fluor-conjugated phalloidin (647 nm) was used as an actin filament marker (1/600 dilution). Slides were imaged in Z-series every 1  $\mu$ m with an Olympus FV-1000 confocal microscope (Olympus America Inc., Center Valley, Pennsylvania). Aggregate two-dimensional images of phalloidin and connexin-43 fluorescence were obtained from the 10 middle layers of the Z-stack. Connexin-43 lateralization was analyzed as described (12).

**OPTICAL MAPPING.** The heart was excised and the coronary artery was perfused with Krebs solution

(120 mM NaCl, 4 mM KCl, 1.2 MgSO<sub>4</sub> 0.7 mM, 1.2 KH<sub>2</sub>PO<sub>4</sub>, 25 mM NaHCO<sub>3</sub>, 5.5 mM glucose, 1.25 mM CaCl<sub>2</sub>, and 95% O<sub>2</sub>/5% CO<sub>2</sub>) at 10 ml/min and 37°C. After 30 min for stabilization and electrical/mechanical decoupling with blebbistatin (15  $\mu$ M), the heart was loaded with di-4-ANEPPS (Biotium, Inc., Hayward, California). A charge-coupled device (CardioCCD, RedShirtImaging, LLC, Decatur, Georgia) was used to record RA free wall fluorescence at 2 kHz. Bipolar electrodes were used to pace the superior right atrium. Optical maps were obtained during 1.5  $\times$  threshold current 2-ms stimulation. Data were analyzed with custom-written algorithms (details of the methods are given in the [Online Appendix](#)).

**STATISTICAL ANALYSIS.** Data are expressed as mean  $\pm$  SEM except for AF duration, which is expressed as median and interquartile range (25% to 75%). The Fisher exact test was applied to compare AF inducibility. Multiple group comparisons were obtained with an analysis of variance model. Bonferroni-

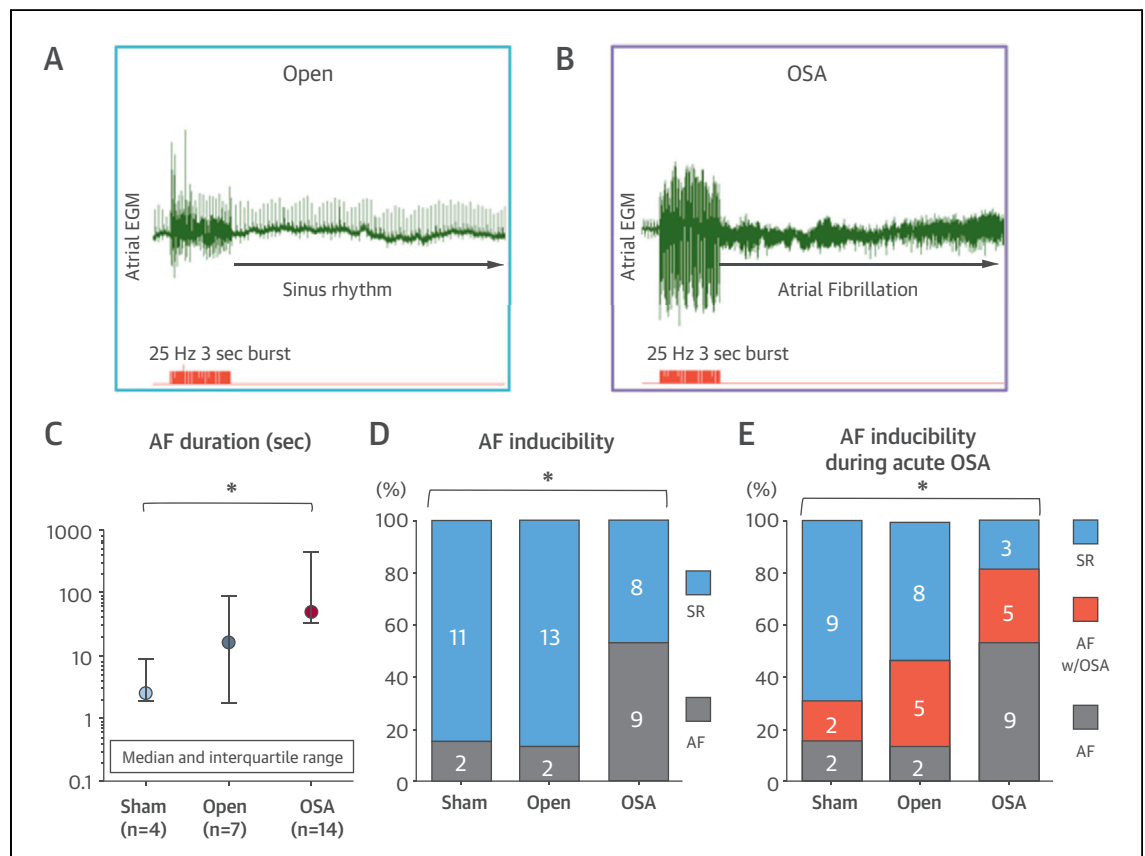


**FIGURE 3 AF Susceptibility Changes at Study End**

Examples of atrial fibrillation (AF) induction attempts in (A) an open airway rat and (B) an OSA rat, respectively. (C) AF duration. (D) AF inducibility. (E) AF inducibility during acute OSA. \* $p < 0.05$  vs. sham. AF duration compared by using 1-way analysis of variance; AF inducibility compared by using the Fisher exact test. EGM = electrogram; OSA = obstructive sleep apnea; SR = sinus rhythm.

corrected Student *t* tests were applied to evaluate individual mean differences when the analysis of variance revealed significant group effects. All data satisfied statistical criteria for normal distribution, except for AF duration, which satisfied normal distribution criteria after logarithmic transformation. Two-tailed *p* values <0.05 were considered significant.

**RESULTS**

**ACUTE RESPONSES TO OSA.** At baseline, esophageal pressure recordings during ventilation were -8.8 ± 0.9 mm Hg, -10.2 ± 0.8 mm Hg, and -9.2 ± 0.9 mm Hg for the sham, open airway, and OSA groups, respectively (*p* = NS). OSA produced acute increases in negative intrathoracic pressure generation (Online Figure 1). Ventilatory arrest with open airways produced much smaller pressure changes. Maximal negative intrathoracic pressure averaged -44.7 ± 2.4 mm Hg in OSA rats versus -16.2 ± 0.4 mm Hg in open airway rats (*p* < 0.001). Correspondingly, acute OSA produced statistically significant LA dilation (Figure 2), which was not seen in other groups. Arterial blood gases confirmed significant oxygen desaturation and hypoventilation in OSA rats (Online Table 1). Open airway rats showed a mild decrease in the partial pressure of oxygen, with no significant desaturation or hypercapnia. During acute OSA, stroke volume decreased, likely because of deep negative intrathoracic pressure. Heart rate also decreased, causing further reductions in cardiac output (Online Figure 2).

**AF SUSCEPTIBILITY CHANGES WITH REPEATED OSA.** Figure 3 shows changes in the AF substrate with repeated OSA over 4 weeks. Burst pacing often failed to induce AF in open airway rats (Figure 3A), while commonly inducing AF in OSA rats (Figure 3B). Mean AF duration increased ~20-fold in chronic OSA rats compared with sham rats (Figure 3C). AF inducibility in the absence of acute OSA was also substantially increased in chronic OSA rats (Figure 3D). We tested AF inducibility in the presence of superimposed acute OSA in rats not inducible at baseline; the goal was to mimic the effect of acute OSA episodes occurring in the presence of cardiac remodeling due to chronic repetitive OSA. Superimposed acute OSA further increased the inducibility of AF, with 5 (62.5%) of 8 previously noninducible chronic OSA rats becoming inducible, versus 5 (38%) of 13 open airway rats and 2 (18%) of 11 sham rats. The result was AF inducibility in a total of 82.4% of chronic OSA rats (Figure 3E).

**CARDIAC REMODELING PRODUCED BY CHRONIC REPETITIVE OSA.** Repetitive OSA clearly produced a substrate for AF susceptibility. Thus, the potential

**TABLE 1 Electrophysiological Variables**

|              | SCL         | SNRT         | WBCL        | aERP       | AVN-ERP    |
|--------------|-------------|--------------|-------------|------------|------------|
| Sham (n = 7) | 193.3 ± 9.7 | 211.4 ± 5.8  | 97.9 ± 2.4  | 34.0 ± 1.0 | 82.9 ± 3.2 |
| Open (n = 8) | 181.6 ± 9.4 | 204.5 ± 12.4 | 103.8 ± 5.7 | 37.0 ± 1.2 | 84.9 ± 4.5 |
| OSA (n =11)  | 180.5 ± 3.2 | 205.3 ± 2.9  | 98.2 ± 1.4  | 35.7 ± 0.6 | 83.8 ± 1.3 |

Values are mean ± SEM and in ms. Comparisons were by 1-way analysis of variance.  
 aERP = atrial effective refractory period; AVN-ERP = atrioventricular node effective refractory period; OSA = obstructive sleep apnea; SCL = sinus node cycle length; SNRT = sinus node recovery time; WBCL = Wenckebach cycle length.

underlying cardiac remodeling changes were examined. There were no significant differences in electrophysiological parameters, including atrial ERP, among the 3 groups (Table 1). Similarly, electrocardiogram parameters did not change between baseline and 4 weeks (Online Table 2). Blood pressure values

**TABLE 2 Echocardiographic Data**

|                         | Sham        | Open        | OSA          |
|-------------------------|-------------|-------------|--------------|
| <b>Baseline (n = 6)</b> |             |             |              |
| LAD, mm                 | 5.26 ± 0.08 | 4.83 ± 0.25 | 4.79 ± 0.25  |
| RAD, mm                 | 4.81 ± 0.16 | 4.54 ± 0.23 | 4.21 ± 0.13  |
| LVAWd, mm               | 1.79 ± 0.05 | 1.79 ± 0.05 | 1.84 ± 0.05  |
| LVPWd, mm               | 1.85 ± 0.07 | 1.74 ± 0.08 | 1.85 ± 0.07  |
| LVDd, mm                | 8.25 ± 0.09 | 7.94 ± 0.15 | 8.08 ± 0.19  |
| LVDs, mm                | 4.38 ± 0.18 | 4.05 ± 0.16 | 4.30 ± 0.11  |
| LVFS, %                 | 47.0 ± 1.8  | 49.0 ± 1.6  | 46.6 ± 2.0   |
| LV mass, mg             | 1073 ± 28   | 981 ± 45    | 1057 ± 26    |
| RVAW, mm                | 0.56 ± 0.06 | 0.55 ± 0.03 | 0.67 ± 0.06  |
| RVD, mm                 | 3.74 ± 0.09 | 3.75 ± 0.09 | 3.24 ± 0.23  |
| Lt PV (S), cm/s         | 51.4 ± 3.5  | 47.3 ± 2.0  | 52.4 ± 2.2   |
| Lt PV (D), cm/s         | 34.5 ± 2.5  | 31.2 ± 2.0  | 31.9 ± 0.7   |
| Lt PV (S/D)             | 0.68 ± 0.05 | 0.73 ± 0.04 | 0.84 ± 0.05  |
| <b>4-week (n = 6)</b>   |             |             |              |
| LAD, mm                 | 5.33 ± 0.10 | 5.36 ± 0.10 | 5.63 ± 0.17  |
| RAD, mm                 | 4.68 ± 0.14 | 4.95 ± 0.24 | 5.09 ± 0.40  |
| LVAWd, mm               | 1.91 ± 0.03 | 1.94 ± 0.04 | 2.00 ± 0.09  |
| LVPWd, mm               | 1.84 ± 0.09 | 1.93 ± 0.08 | 1.94 ± 0.11  |
| LVDd, mm                | 8.23 ± 0.10 | 8.48 ± 0.14 | 8.99 ± 0.22* |
| LVDs, mm                | 4.32 ± 0.11 | 4.08 ± 0.17 | 4.86 ± 0.21† |
| LVFS, %                 | 47.5 ± 1.1  | 51.9 ± 1.6  | 46.1 ± 1.3†  |
| LV mass, mg             | 1107 ± 30   | 1204 ± 51   | 1346 ± 115‡  |
| RVAW, mm                | 0.61 ± 0.06 | 0.70 ± 0.05 | 0.88 ± 0.09* |
| RVD, mm                 | 3.76 ± 0.15 | 3.80 ± 0.26 | 3.69 ± 0.25  |
| Lt PV (S), cm/s         | 50.8 ± 3.2  | 47.0 ± 2.1  | 40.8 ± 4.0   |
| Lt PV (D), cm/s         | 30.7 ± 2.6  | 30.2 ± 1.5  | 30.4 ± 0.7   |
| Lt PV (S/D)             | 1.67 ± 0.09 | 1.56 ± 0.04 | 1.34 ± 0.11* |

Values are mean ± SEM. \**p* <0.01 vs sham (4-week), by 1-way analysis of variance/Bonferroni-adjusted Student *t* tests. †*p* < 0.05 vs sham (4-week). ‡*p* <0.05 vs open (4-week).  
 D = diastolic; LAD = left atrial diameter; Lt = left; LV = left ventricular; LVAWd = left ventricular anterior wall thickness; LVDd = left ventricular dimension in diastole; LVDs = left ventricular dimension in systole; LVFS = left ventricular fractional shortening; LVPWd = left ventricular posterior wall thickness; OSA = obstructive sleep apnea; PV = pulmonary venous flow; RAD = right atrial diameter; RV = right ventricular; RVAW = right ventricular anterior wall thickness; RVD = right ventricular dimension; S = systolic; S/D = systolic/diastolic pulmonary venous flow ratio.



at end of study did not differ among groups (Online Table 3). However, echocardiography revealed significant LV remodeling in chronic OSA rats (Table 2). Statistically significant increases in LV diameter and LV mass occurred, indicating eccentric hypertrophy. Right ventricular (RV) anterior wall thickness also increased, and the pulmonary venous systolic/diastolic flow ratio decreased, indicating LV diastolic dysfunction. LV systolic function (as indicated by LV fractional shortening) did not change. The heart weight/body weight ratio was significantly increased in chronic OSA rats (sham  $2.69 \pm 0.05$  mg/g; open  $2.63 \pm 0.06$  mg/g; OSA  $2.91 \pm 0.05$  mg/g;  $p < 0.005$  vs open

and sham). There were no long-term effects of repetitive OSA on cardiac output (Online Figure 3).

Because atrial refractoriness did not change, we wondered whether chronic OSA might be causing conduction changes predisposing to reentry. Optical mapping was therefore performed to precisely assess conduction. Figure 4A shows activation maps from each group. These were subjected to detailed quantitative conduction velocity analysis (Online Appendix), which revealed highly significant conduction slowing in chronic OSA rats (Figure 4B).

**CONNEXIN CHANGES AND FIBROSIS.** To understand the mechanisms underlying the conduction slowing caused by repetitive OSA, we analyzed changes in connexin expression and fibrous tissue content. Mild, but statistically significant, fibrosis occurred in OSA rats (Online Figure 4). Because the extent of fibrosis seemed insufficient to explain the conduction changes in OSA rats, other possibilities were analyzed, including altered  $\text{Na}^+$ -channel subunit expression and connexin changes. Although  $\text{Na}^+$ -channel alpha subunit gene expression was unaffected by OSA (Online Figure 5), connexin-43 showed substantial remodeling. Figure 5A presents images of immunofluorescence staining of connexin-43 from LA tissue, which was reduced in OSA rats. Quantitative analysis is presented in Figure 5B and indicates a statistically significant reduction of ~58% in OSA rats. Furthermore, there was substantial connexin redistribution to lateral cell margins in OSA rats (Figure 5C). Neither connexin-40 nor phosphoconnexin-43 antibodies provided resolvable immunofluorescence signals.

We pursued the analysis of connexin expression by using Western blots. Figure 6A shows bands corresponding to total and ser368-phosphorylated connexin-43, with quantitative analyses presented in Figure 6B. Total connexin-43 expression in chronic OSA rats was less than in sham rats, and qualitatively similar to the immunofluorescence data in Figure 5B. Phosphorylated connexin expression was quantitatively smaller in both open airway and OSA rats, with wide variation and no statistically significant differences among groups. Consistent with previous observations of extremely weak connexin-40 expression in rat atria (12), connexin-40 was not detectable (Online Figure 6). Finally, we examined potential mechanisms underlying connexin changes. Previous evidence pointed to p38-MAPK regulation of connexin expression (13). Figure 6A shows Western blots for total and phosphorylated p38-MAPK, with corresponding quantitative data presented in Figure 6C. The p38-MAPK phosphorylation ratios were significantly increased in both the open airway

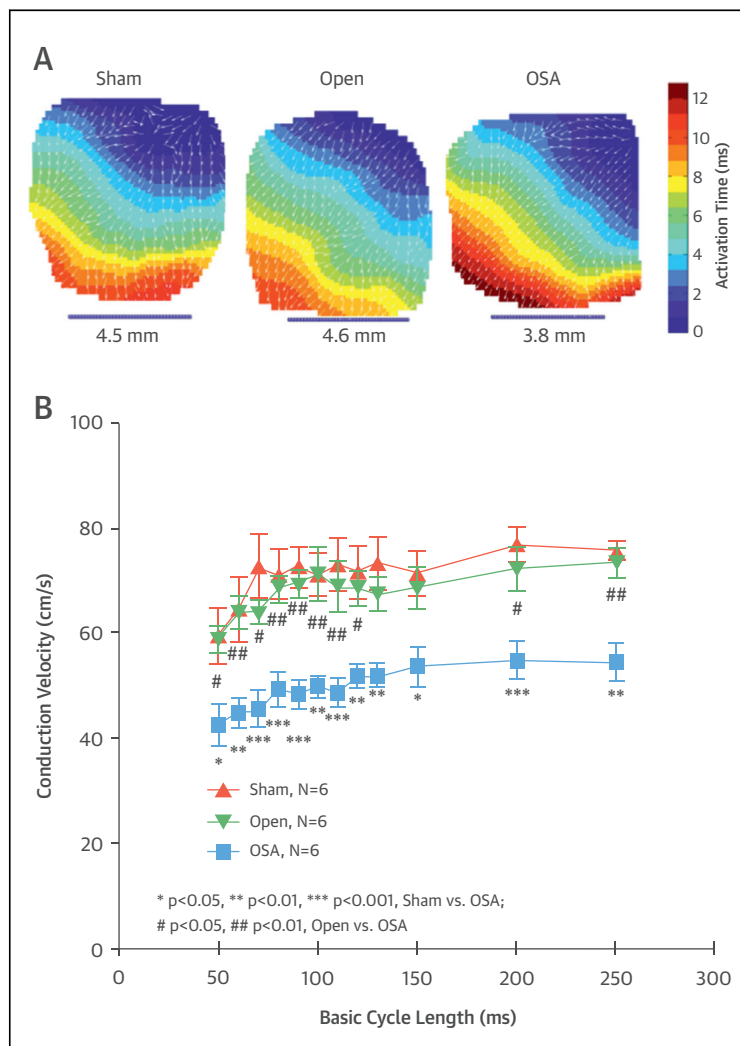


**FIGURE 4** Optical Mapping Data

(A) Examples of right atrial activation maps from each group, with conduction vectors shown as small white arrows. (B) Mean  $\pm$  SEM conduction velocity data. Comparisons were made by using 2-way repeated-measures analysis of variance/Bonferroni-adjusted Student t tests. OSA = obstructive sleep apnea.

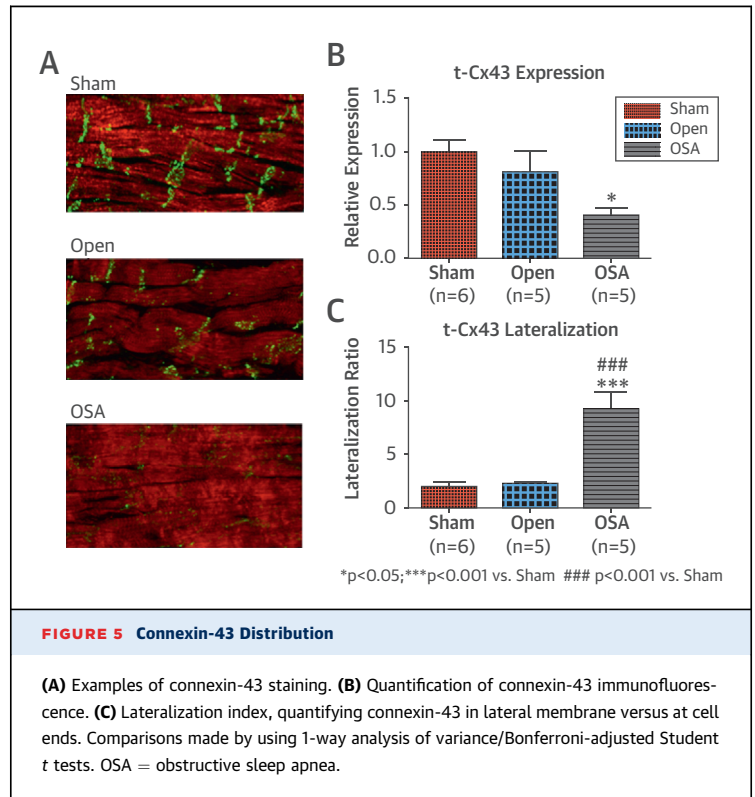
and OSA rats. No changes in ERK expression or phosphorylation were noted (Online Figure 7).

## DISCUSSION

The present study represents the first experimental analysis of the effects of long-term repetitive OSA on the cardiac substrate for AF, to our knowledge. We found substantial increases in AF vulnerability, including increased duration and inducibility of AF. Underlying remodeling included atrial conduction slowing, with no changes in atrial refractoriness. Conduction slowing was accompanied by important changes in atrial connexin-43 expression and distribution, along with modest, but statistically significant, increases in atrial fibrous tissue content. In addition, cardiac structure/function remodeling was seen in terms of LV dilation, hypertrophy, and diastolic dysfunction, along with RV hypertrophy.

**COMPARISON WITH PREVIOUS ANIMAL STUDIES AND CONSIDERATIONS OF THE MODEL.** A variety of animal studies have explored the atrial arrhythmogenic properties of acute OSA (5,9,14,15). Autonomic nervous system activation, particularly of the vagal component, plays an important role. However, acute LA dilation/stretch caused by increased venous return due to negative intrathoracic pressures also contributes (9). Severe hypercapnia alters atrial electrophysiology, both lengthening atrial ERP and prolonging conduction time, whereas hypoxia has limited effects (16).

The present study is, to the best of our knowledge, the first animal investigation to examine the effects of chronic repetitive OSA, as typically occurs in patients, on the substrate for AF. Our rats were exposed to 20 cycles of obstructive apnea per day, achieving negative intrathoracic pressures of about -50 mm Hg, which is similar to the clinically observed levels of about -65 mm Hg achieved in patients (17). We found that chronic repetitive OSA produces a vulnerable substrate for AF, with both ventricular function changes (predominantly diastolic dysfunction) and prominent conduction disturbances. Taken together with our previous study of acute OSA (9), our results point to complex AF pathophysiology in OSA syndrome (Central Illustration). Acute OSA promotes AF inducibility via autonomic changes and acute LA stretch. However, in our previous study, acute OSA alone did not increase AF duration and produced AF inducibility in only a minority of lean rats. By adding diastolic dysfunction that enhanced LA dilation under OSA conditions, obesity substantially increased AF inducibility with acute OSA. The cardiac remodeling resulting from repetitive OSA in the present



study clearly had an AF-promoting effect, even in the absence of acute OSA, with prolonged AF duration and increased AF inducibility (Figures 3C and 3D). When exposed to acute OSA, chronic OSA rats displayed further increased AF inducibility (Figure 3E). Thus, the atrial remodeling and cardiac function disturbances caused by repetitive OSA episodes are themselves arrhythmogenic but also sensitize the heart to the immediate AF-promoting effects of acute OSA (Central Illustration).

**RELATIONSHIP TO CLINICAL OBSERVATIONS AND POTENTIAL IMPORTANCE.** The AF-promoting effects of OSA in humans are well established (18). The presence and severity of OSA predict AF recurrences in patients taking antiarrhythmic drugs (19,20) and after AF ablation (21). Furthermore, OSA treatment with continuous positive airway pressure reduces recurrence rates after AF ablation (22).

Recent studies have demonstrated significant cardiac remodeling in patients with OSA. OSA augments atrial electromechanical delay and P-wave dispersion, which increase with OSA severity (23). Patients with OSA exhibit prolonged atrial conduction times, longer P waves, slowed atrial conduction velocities, lower atrial electrogram voltages, and more complex electrograms (11,24). Signal-averaged P-wave duration is increased by OSA and significantly decreases

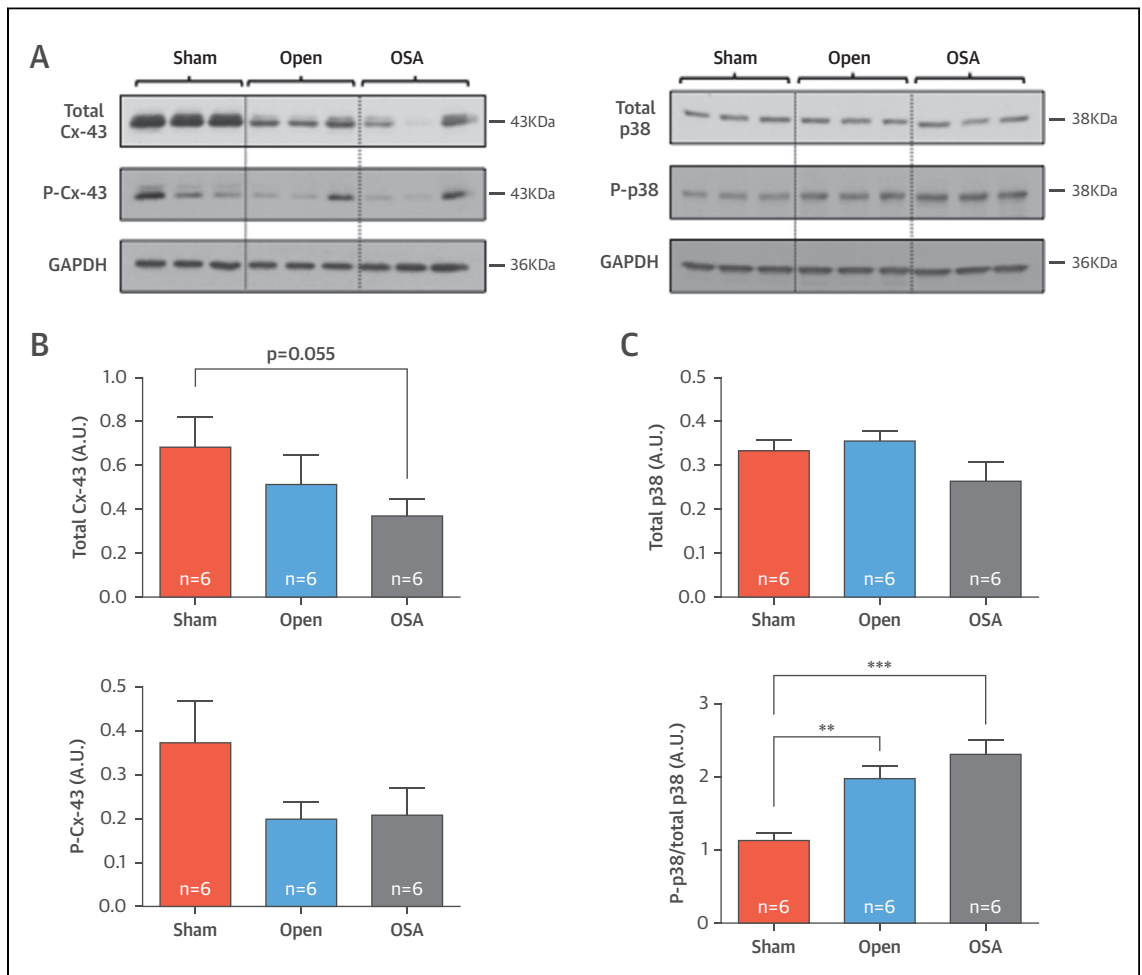


**FIGURE 6** Western-Blot Quantification of Connexin-43 and p38-MAPK

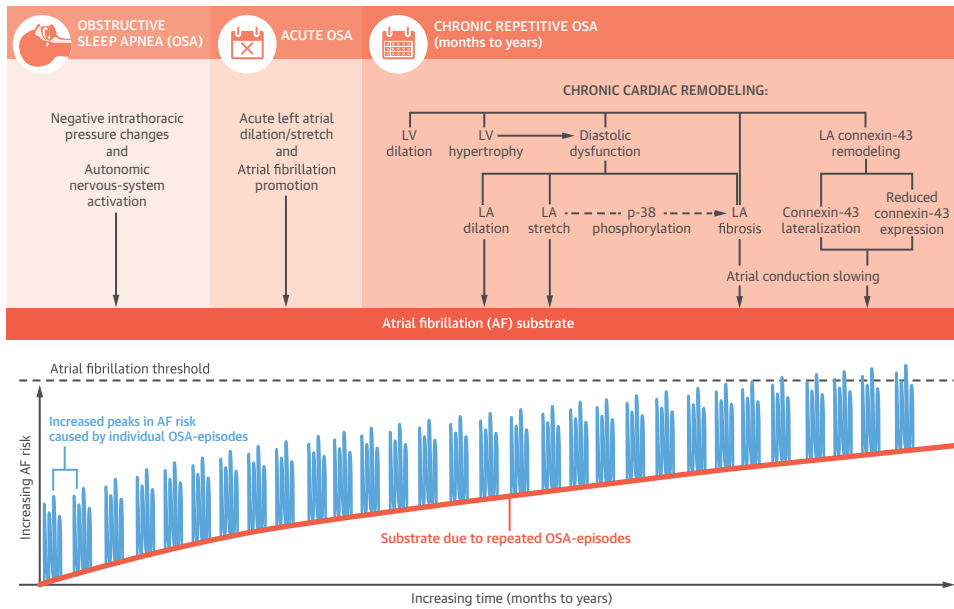
(A) Representative Western blots for total and Ser368-phosphorylated connexin-43 (left) and total and Thr180/Tyr182-diphosphorylated p38 (right) along with glyceraldehyde-3-phosphate dehydrogenase (GAPDH). (B) Quantification of total (top) and phosphorylated (bottom) connexin-43. (C) Quantification of total p38 (top) and phosphorylation ratio (phosphorylated-p38/total-p38) (bottom). \* $p < 0.05$ , \*\* $p < 0.01$ , \*\*\* $p < 0.001$ .  $n = 6$  per group by 1-way analysis of variance/Bonferroni-adjusted Student  $t$  tests. MAPK = mitogen-activated protein kinase; OSA = obstructive sleep apnea.

with continuous positive airway pressure treatment (25). OSA is also associated with LV hypertrophy and dilation, as well as an increased risk of systolic dysfunction (26).

Our findings are consistent with and shed light on clinical observations. In clinical databases, it is difficult to determine whether OSA directly causes cardiac remodeling or whether the observed associations are due to related conditions such as obesity. We found that repeated OSA episodes are sufficient to induce significant atrial conduction abnormalities, to enhance AF susceptibility, and to produce LV and RV hypertrophy, LV dilation, and diastolic dysfunction. Furthermore, our results provide insights into the mechanisms underlying AF-promoting conduction

disturbances, including extensive connexin remodeling and increased atrial fibrous tissue content. In addition to providing insights into mechanisms, our results have relevance to therapeutic approaches. Atrial fibrosis reverses slowly, if at all (27); therefore, to prevent the development of irreversible components of the substrate, it may be important to treat OSA as promptly as possible. In addition, gene transfer approaches have demonstrated the feasibility of restoring connexins in paradigms involving AF related to impaired connexin expression (28,29). These observations highlight the possibility of mechanism-targeted therapy of AF associated with conduction disorders, if the underlying basis can be identified.





Iwasaki, Y., et al., J Am Coll Cardiol. 2014; 64(19):2013-23.

**CENTRAL ILLUSTRATION** Mechanisms by Which OSA Leads to AF

**(Top)** Acute obstructive sleep apnea (OSA) episodes promote atrial fibrillation (AF) via left atrial (LA) dilation and stretch (**second box**). However, for AF to be manifest, an underlying substrate is needed. Chronic repetitive OSA episodes lead to an AF substrate by the mechanisms shown in the **third box**. Repeated OSA produces cardiac remodeling, including left ventricular (LV) dilation and hypertrophy. LV hypertrophy causes diastolic dysfunction. Diastolic dysfunction leads to LA dilation, stretch, and fibrosis. LA stretch causes phosphorylation of the mitogen-activated protein kinase p-38, which promotes fibrosis. In addition, LA connexin-43 expression is altered, with both reduced levels and displacement of the connexins from the cell ends (where they mediate cell-to-cell coupling) to the lateral cell margins. LA fibrosis and LA connexin changes, in combination with LA dilation and stretch, produce an AF substrate. **(Bottom)** Illustration of how OSA causes AF. Individual acute episodes raise AF risk (**blue lines**), but in the absence of an underlying AF-prone substrate, they are not enough to reach the threshold (**dashed black line**) necessary to cause AF occurrence. Over longer periods (months to years), repeated OSA episodes induce cardiac remodeling that produces a substrate for AF (**red line**); therefore, the AF risk increase caused by individual OSA episodes reaches the threshold and causes clinical AF. Acute OSA episodes can then readily trigger AF episodes in the presence of the substrate caused by cardiac remodeling that was triggered by previous repeated OSA episodes.

**MECHANISTIC INSIGHTS.** We identified a number of aspects of cardiac remodeling caused by repetitive OSA that likely contribute to the enhanced AF susceptibility that we noted. Atrial fibrosis is a known profibrillatory substrate (30). However, although the fibrosis we observed in the present model was statistically significant, it remained relatively modest: ~70% increase compared with the 16-fold increase underlying the AF substrate in a canine congestive heart failure model (31). The precise relationship between fibrosis extent and AF promotion is unclear; therefore, despite its relatively modest nature, fibrosis might have contributed to the AF seen with repeated OSA. However, there is extensive evidence for important contributions of connexin remodeling to the AF substrate (32), suggesting that the connexin changes we observed played a significant role. As

such, the present findings provide a new, clinically relevant paradigm for the contribution of connexin changes to AF. In addition to electrophysiological remodeling, the contribution of altered cardiac hemodynamic function to OSA-associated AF should not be overlooked. The LV dysfunction we noted likely participated, particularly by enhancing the LA stretch during acute OSA, as we reported previously with LV hypertrophy and diastolic dysfunction resulting from obesity (9).

**STUDY LIMITATIONS.** The biological factors connecting repetitive OSA to atrial remodeling must still be determined. OSA causes acute LA stretch, and repeated stretch is a major contributor to atrial remodeling associated with AF (33). Stretch causes p38-MAPK phosphorylation, which activates fibroblasts and promotes fibrosis (34). We observed

increased p38 phosphorylation with OSA, which might have contributed to its fibrogenic properties. The mechanisms that might underlie connexin-43 changes with OSA and the effects of MAPKs are somewhat unclear. Some studies show that p38 and ERK MAPK activation enhance connexin expression (13,35), whereas others suggest that p38 MAPK activation impairs connexin-43 phosphorylation and gap junction conductance (36). Myocardial stretch may also have complex effects, with in vitro stretch enhancing connexin-43 expression but in vivo stretch reducing it (37). Hypoxia itself slowly and reversibly down-regulates connexin-43 expression (38). Inflammatory pathways could also be involved. There is also evidence for roles of hypercapnia in both acute AF-promoting effects of OSA (16) and sympathetic activation (39), which could have contributed to long-term remodeling. Clearly, more work is needed to understand the molecular basis of cardiac remodeling caused by repetitive OSA. The model developed here may be valuable for the systematic mechanistic analyses needed.

Like all animal models of human disease, the model we developed here is not a perfect counterpart of any human condition. It does provide insights into the cardiac remodeling caused by repetitive obstructive apnea, and shows that this remodeling produces a substrate that can maintain AF. Clinical investigation is needed to validate the applicability of our findings to humans. Further work in this and other animal models will also be necessary to go further in establishing the basic mechanisms coupling sleep apnea to proarrhythmic cardiac remodeling.

## CONCLUSIONS

We successfully developed an animal model of AF promotion due to repetitive OSA, which displays

many of the clinical features seen in patients with OSA-related AF. The AF-associated substrate includes atrial conduction slowing due to connexin remodeling and atrial fibrosis, along with OSA-induced ventricular function changes. This work provides insights into mechanisms underlying an important clinical problem, as well as a novel model that can be used for further mechanistic exploration.

**ACKNOWLEDGMENTS** The authors thank Nathalie L'Heureux, Chantal St-Cyr, and Audrey Bernard for technical help and France Thériault for secretarial assistance.

**REPRINT REQUESTS AND CORRESPONDENCE:** Dr. Stanley Nattel, Montréal Heart Institute, 5000 Belanger Street East, Montreal, Quebec H1T 1C8, Canada. E-mail: [stanley.nattel@icm-mhi.org](mailto:stanley.nattel@icm-mhi.org).

## PERSPECTIVES

**COMPETENCY IN MEDICAL KNOWLEDGE:** In a rat model, repetitive episodes of sleep apnea are associated with left ventricular diastolic dysfunction and dilation, atrial fibrosis, and disruption of the atrial connexin proteins. These factors could contribute to the development of atrial fibrillation.

**TRANSLATIONAL OUTLOOK:** The development of treatments that prevent or reverse substrate changes in the atria by inhibiting atrial fibrosis, improving intercellular electrical communication, or restoring normal atrial connexin expression and distribution may reduce the incidence of atrial fibrillation in patients with sleep apnea.

## REFERENCES

- Young T, Palta M, Dempsey J, et al. The occurrence of sleep-disordered breathing among middle-aged adults. *N Engl J Med* 1993;328:1230-5.
- Gami AS, Pressman G, Caples SM, et al. Association of atrial fibrillation and obstructive sleep apnea. *Circulation* 2004;110:364-7.
- Gami AS, Hodge DO, Herges RM, et al. Obstructive sleep apnea, obesity, and the risk of incident atrial fibrillation. *J Am Coll Cardiol* 2007;49:565-71.
- Tkacova R, Rankin F, Fitzgerald FS, et al. Effects of continuous positive airway pressure on obstructive sleep apnea and left ventricular afterload in patients with heart failure. *Circulation* 1998;98:2269-75.
- Linz D, Schotten U, Neuberger HR, et al. Negative tracheal pressure during obstructive respiratory events promotes atrial fibrillation by vagal activation. *Heart Rhythm* 2011;8:1436-43.
- Roche F, Xuong AN, Court-Fortune I, et al. Relationship among the severity of sleep apnea syndrome, cardiac arrhythmias, and autonomic imbalance. *Pacing Clin Electrophysiol* 2003;26:669-77.
- Fung JW, Li TS, Choy DK, et al. Severe obstructive sleep apnea is associated with left ventricular diastolic dysfunction. *Chest* 2002;121:422-9.
- Myslinski W, Duchna HW, Rasche K, et al. Left ventricular geometry in patients with obstructive sleep apnea coexisting with treated systemic hypertension. *Respiration* 2007;74:176-83.
- Iwasaki Y-K, Shi Y, Benito B, et al. Determinants of atrial fibrillation in an animal model of obesity and acute obstructive sleep apnea. *Heart Rhythm* 2012;9:1409-16.e1.
- Baguet JP, Barone-Rochette G, Tamisier R, et al. Mechanisms of cardiac dysfunction in obstructive sleep apnea. *Nat Rev Cardiol* 2012;9:679-88.
- Dimitri H, Ng M, Brooks AG, et al. Atrial remodeling in obstructive sleep apnea: implications for atrial fibrillation. *Heart Rhythm* 2012;9:321-7.
- Gros D, Jarry-Guichard T, Ten Velde I, et al. Restricted distribution of connexin40, a gap junctional protein, in mammalian heart. *Circ Res* 1994;74:839-51.
- Inoue N, Ohkusa T, Nao T, et al. Rapid electrical stimulation of contraction modulates gap junction protein in neonatal rat cultured cardiomyocytes: involvement of mitogen-activated protein kinases and effects of angiotensin

- II-receptor antagonist. *J Am Coll Cardiol* 2004;44:914-22.
14. Ghias M, Scherlag BJ, Lu Z, et al. The role of ganglionated plexi in apnea-related atrial fibrillation. *J Am Coll Cardiol* 2009;54:2075-83.
15. Linz D, Hohl M, Nickel A, et al. Effect of renal denervation on neurohumoral activation triggering atrial fibrillation in obstructive sleep apnea. *Hypertension* 2013;62:767-74.
16. Stevenson IH, Roberts-Thomson KC, Kistler PM, et al. Atrial electrophysiology is altered by acute hypercapnia but not hypoxemia: implications for promotion of atrial fibrillation in pulmonary disease and sleep apnea. *Heart Rhythm* 2010;7:1263-70.
17. Somers VK, White DP, Amin R, et al. Sleep apnea and cardiovascular disease: an American Heart Association/American College of Cardiology Foundation Scientific Statement from the American Heart Association Council for High Blood Pressure Research Professional Education Committee, Council on Clinical Cardiology, Stroke Council, and Council on Cardiovascular Nursing. *J Am Coll Cardiol* 2008;52:686-717.
18. Digby GC, Baranchuk A. Sleep apnea and atrial fibrillation; 2012 update. *Curr Cardiol Rev* 2012;8:265-72.
19. Monahan K, Brewster J, Wang L, et al. Relation of the severity of obstructive sleep apnea in response to anti-arrhythmic drugs in patients with atrial fibrillation or atrial flutter. *Am J Cardiol* 2012;110:369-72.
20. Ng CY, Liu T, Shehata M, et al. Meta-analysis of obstructive sleep apnea as predictor of atrial fibrillation recurrence after catheter ablation. *Am J Cardiol* 2011;108:47-51.
21. Naruse Y, Tada H, Satoh M, et al. Concomitant obstructive sleep apnea increases the recurrence of atrial fibrillation following radiofrequency catheter ablation of atrial fibrillation: clinical impact of continuous positive airway pressure therapy. *Heart Rhythm* 2013;10:331-7.
22. Fein AS, Shvilkin A, Shah D, et al. Treatment of obstructive sleep apnea reduces the risk of atrial fibrillation recurrence after catheter ablation. *J Am Coll Cardiol* 2013;62:300-5.
23. Cagirci G, Cay S, Gulsoy KG, et al. Tissue Doppler atrial conduction times and electrocardiogram interlead P-wave durations with varying severity of obstructive sleep apnea. *J Electrocardiol* 2011;44:478-82.
24. Maeno K, Kasai T, Kasagi S, et al. Relationship between atrial conduction delay and obstructive sleep apnea. *Heart Vessels* 2013;28:639-45.
25. Maeno K, Kasagi S, Ueda A, et al. Effects of obstructive sleep apnea and its treatment on signal-averaged P-wave duration in men. *Circ Arrhythm Electrophysiol* 2013;6:287-93.
26. Chami HA, Devereux RB, Gottdiener JS, et al. Left ventricular morphology and systolic function in sleep-disordered breathing: the Sleep Heart Health Study. *Circulation* 2008;117:2599-607.
27. Shinagawa K, Shi YF, Tardif JC, et al. Dynamic nature of atrial fibrillation substrate during development and reversal of heart failure in dogs. *Circulation* 2002;105:2672-8.
28. Igarashi T, Finet JE, Takeuchi A, et al. Connexin gene transfer preserves conduction velocity and prevents atrial fibrillation. *Circulation* 2012;125:216-25.
29. Bikou O, Thomas D, Trappe K, et al. Connexin 43 gene therapy prevents persistent atrial fibrillation in a porcine model. *Cardiovasc Res* 2011;92:218-25.
30. Iwasaki YK, Nishida K, Kato T, et al. Atrial fibrillation pathophysiology: implications for management. *Circulation* 2011;124:2264-74.
31. Li D, Fareh S, Leung TK, et al. Promotion of atrial fibrillation by heart failure in dogs: atrial remodeling of a different sort. *Circulation* 1999;100:87-95.
32. Kato T, Iwasaki YK, Nattel S. Connexins and atrial fibrillation: filling in the gaps. *Circulation* 2012;125:203-6.
33. De Jong AM, Maass AH, Oberdorf-Maass SU, et al. Mechanisms of atrial structural changes caused by stretch occurring before and during early atrial fibrillation. *Cardiovasc Res* 2011;89:754-65.
34. Du QC, Zhang DZ, Chen XJ, et al. The effect of p38MAPK on cyclic stretch in human facial hypertrophic scar fibroblast differentiation. *PLoS One* 2013;8:e75635.
35. Polontchouk L, Ebelt B, Jackels M, et al. Chronic effects of endothelin 1 and angiotensin II on gap junctions and intercellular communication in cardiac cells. *FASEB J* 2002;16:87-9.
36. Ogawa T, Hayashi T, Kyoizumi S, et al. Anisomycin downregulates gap-junctional intercellular communication via the p38 MAP-kinase pathway. *J Cell Sci* 2004;117:2087-96.
37. Hussain W, Patel PM, Chowdhury RA, et al. The renin-angiotensin system mediates the effects of stretch on conduction velocity, connexin43 expression, and redistribution in intact ventricle. *J Cardiovasc Electrophysiol* 2010;21:1276-83.
38. Severino A, Narducci ML, Pedicino D, et al. Reversible atrial gap junction remodeling during hypoxia/reoxygenation and ischemia: a possible arrhythmogenic substrate for atrial fibrillation. *Gen Physiol Biophys* 2012;31:439-48.
39. Somers VK, Mark AL, Zavala DC, et al. Contrasting effects of hypoxia and hypercapnia on ventilation and sympathetic activity in humans. *J Appl Physiol* (1985) 1989;67:2101-6.

---

**KEY WORDS** atrial fibrosis, cardiac arrhythmia mechanisms, diastolic dysfunction, electrocardiogram, obstructive sleep apnea

---

**APPENDIX** For an expanded Methods section as well as supplemental tables and figures, please see the online version of this article.